

# RSC Advances



This article can be cited before page numbers have been issued, to do this please use: K. Siva, S. Kalainathan, M. Yamada, Y. Kondo and F. Hamada, *RSC Adv.*, 2016, DOI: 10.1039/C6RA05055G.



This is an *Accepted Manuscript*, which has been through the Royal Society of Chemistry peer review process and has been accepted for publication.

*Accepted Manuscripts* are published online shortly after acceptance, before technical editing, formatting and proof reading. Using this free service, authors can make their results available to the community, in citable form, before we publish the edited article. This *Accepted Manuscript* will be replaced by the edited, formatted and paginated article as soon as this is available.

You can find more information about *Accepted Manuscripts* in the [Information for Authors](#).

Please note that technical editing may introduce minor changes to the text and/or graphics, which may alter content. The journal's standard [Terms & Conditions](#) and the [Ethical guidelines](#) still apply. In no event shall the Royal Society of Chemistry be held responsible for any errors or omissions in this *Accepted Manuscript* or any consequences arising from the use of any information it contains.

# Synthesis, growth and third-order nonlinear optical properties of quinolinium single crystal-PCLQI

S. Karthiga, S. Kalainathan\*, Fumio Hamada<sup>1</sup>, Manabu Yamada<sup>2</sup>, Yoshihiko Kondo<sup>3</sup>.

*Centre for Crystal Growth, School of Advanced Sciences, VIT University, Vellore- 632014, Tamil Nadu*

<sup>1</sup>*Department of Applied Chemistry for Environments, Graduate School of Engineering and Resource Science, Akita University, 1-1 Tegatagakuen-machi, Akita, 010-8502, Japan.*

<sup>2</sup>*Research Center for Engineering Science, Graduate School of Engineering and Resource Science, Akita University, 1-1 Tegatagakuen-machi, Akita, 010-8502, Japan.*

<sup>3</sup>*Department of Life Science, Graduate School of Engineering and Resource Science, Akita University, 1-1 Tegatagakuen-machi, Akita, 010-8502, Japan.*

## Abstract

N-ethyl quinolinium chromophore crystal 2-[2-(4-Chloro-phenyl)-vinyl]-1-ethyl-quinolinium iodide (PCLQI) has been successfully grown by slow evaporation technique. Single crystal X-ray diffraction studies revealed that the title compound crystallizes in monoclinic crystal system with centrosymmetric space group C2/c. The molecular formation of the grown crystal was initially identified using <sup>1</sup>H NMR and FTIR analysis. The linear optical studies of the title crystal were done by UV-vis-NIR studies and the thermal studies revealed the stability of the title material till its melting point 239.7 °C. The grown crystal exhibited high third order optical nonlinearity which was determined by Z-Scan technique.

## 1. Introduction

Organic nonlinear optical materials with high second order optical nonlinearities have attracted much attention for potential applications in various fields such as THz generation, opto electronics, optical frequency conversion, photonics and integrated optics applications [1 - 3]. The ionic organic NLO crystals are attractive materials for second order nonlinear

applications [4, 5] due to the presence of delocalized  $\pi$  electrons and coulombic interactions [6-8]. The ionic stilbazolium derivatives, have led to many breakthrough in macroscopic nonlinearities as well as crystal characteristics. Organic ionic crystals are interesting because they exhibits large NLO properties, posses an easy tunability by changing the counter ion to crystallize into non centrosymmetric structure [9] and the best combination of donor and acceptor groups provides a better enhancement. Non centrosymmetric hetero aromatic pyridinium cations exhibit excellent nonlinear optical properties due to their large first order hyperpolarizability. Therefore, the electron withdrawing strength of electron acceptor group is most important to obtain desired optical properties for many applications [10]. One strategy to enhance the electron withdrawing strength and hyperpolarizability of the cation is by elongation of its  $\pi$ - conjugated system. Vladimir et al. have depicted the crystal structure for a new family of quinolinium derived acentric materials, which exhibits high hyperpolarizability combined with a noncentrosymmetric structure [11]. Recently, a quinolinium acceptor group with strong  $\pi$ -conjugated system has been introduced, which exhibits a large molecular hyperpolarizability and large macroscopic nonlinear optical response [12, 13]. For example, HMQ-T and HMQ-MBS exhibit high order parameter and large optical nonlinearity in the range of benchmark stilbazolium DAST crystal [14]. Recently, many quinolinium chromophores have been synthesized and widely investigated by many research groups by changing the anionic group (aryl sulfonate) to create new molecules with a large NLO response. However, higher molecular polarizability leads to intensive dipole-dipole interactions that tends the chromophores to compensate the total dipole moment by packing in more centrosymmetric structures in organic molecules, which significantly enhances the third-order nonlinear optical property of the materials [11]. Various ionic organic crystals chromophore arranged in centrosymmetric manner posses third harmonic generation [15] which are being perform effectively in information processing devices. The prerequisite for a

third order chromophore is to have high thermal stability, good transparency, high non-linearity and process ability. These motivated us to synthesis and investigate the third order optical nonlinearity of quinolinium derived single crystals and to find application in the fields of optical switching and optical limiting devices [16].

Here in we report a new organic material 2-[2-(4-Chloro-phenyl)-vinyl]-1-ethyl-quinolinium iodide, which is a series of  $\pi$ -conjugated styryl quinolinium chromophore from the stilbene family. Third order optical property were analysed by using Z- scan technique, which reveal that the PCLQI crystal shows high nonlinear absorption coefficient, making them potential candidate for optoelectronic and optical switching applications. Further, grown crystal was investigated by various instrumentation techniques to analyse their structural and optical properties and to check their suitability for device fabrication.

## 2. Experimental procedure

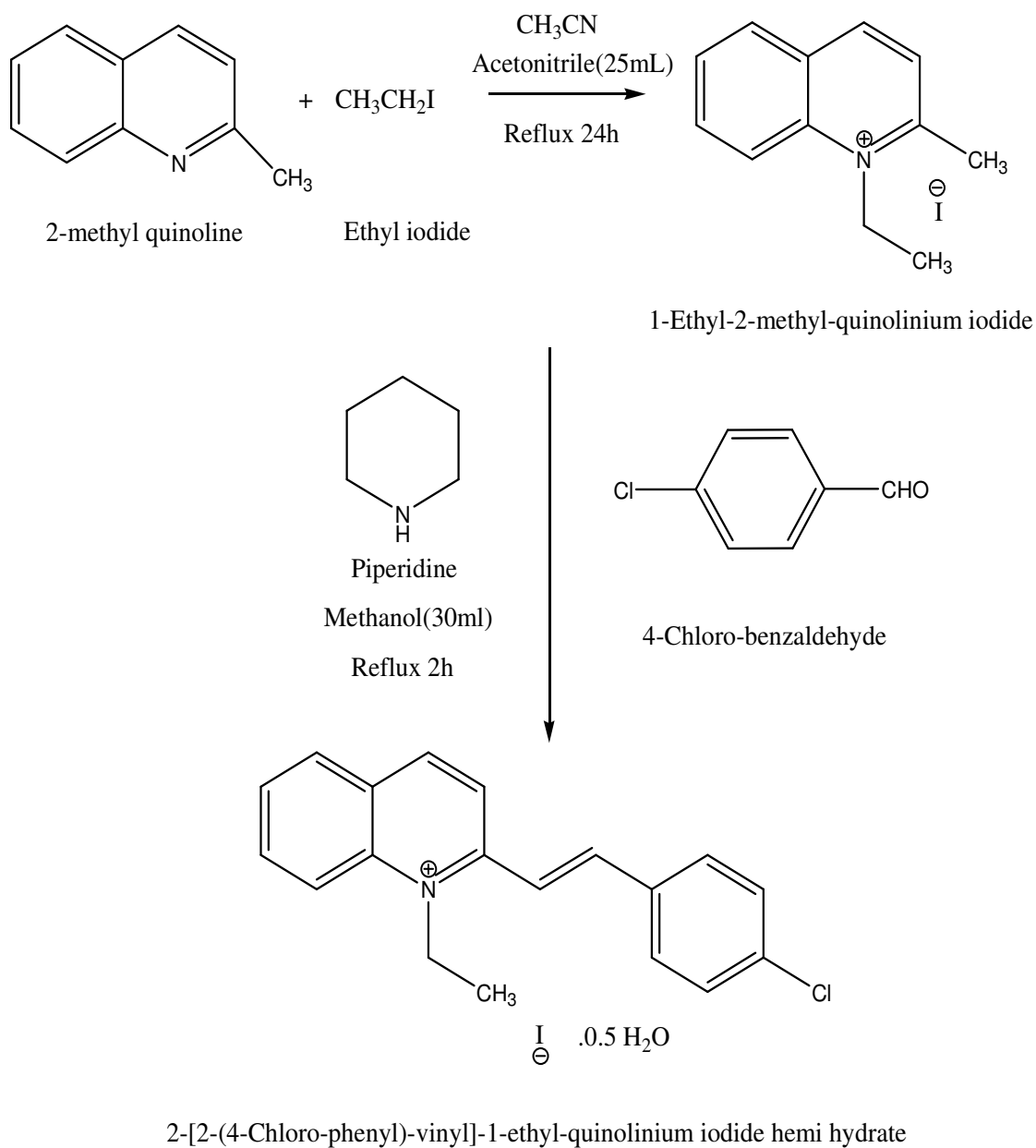
### 2.1 Material synthesis

All high purity chemical reagents and solvents were purchased from Alfa Aesar and Sigma Aldrich and used for synthesis without further purification. The overall synthesis process of starting material involving two- step synthesis route were shown in scheme 1.

**1-Ethyl-2-methyl-quinolinium iodide (1)** : 1-Ethyl-2-methyl-quinolinium iodide was synthesized by taking a solution of 2-methyl quinoline (1mmol) and ethyl iodide (3mmol) in acetonitrile (25ml). The mixture were heated under reflux for 24h and cooled to ambient temperature. After cooling diethyl ether was added, the desired quaternary ammonium salt was collected by filtration. The ether from the combined filtrate was removed by evaporation and the remaining residue, consisting mainly of the unreacted starting material, was heated under reflux for another 24h and the steps are repeated as mentioned above. The obtained

pale yellow salt was dried in an oven. The process was repeated several times to achieve a suitable yield.

**2-[2-(4-Chloro-phenyl)-vinyl]-1-ethyl-quinolinium iodide (2):** The title material PCLQI (**2**) was prepared by taking stoichiometric ratio of 1-Ethyl-2-methyl-quinolinium iodide (**1**) (0.89g, 3mmol) and p-chloro benzaldehyde (0.42g, 3mmol) in methanol (30mL) and piperidine added as a catalyst (few drops). The above mixtures were taken in a 250mL round bottom flask and the mixture solution was refluxed for 2h. The resulted brown solid was filtered off and washed 3-5 times with Diethyl ether to remove unreacted starting materials. The purity of the title compound (**2**) was increased by repeated recrystallization from methanol.



Scheme 1: Synthesis of PCLQI

## 2.2 Solubility, crystal growth and morphology

The solubility test plays an important role in deciding the best solvent and temperature to grow good quality crystals. The solubility measurement provides information about the nucleation and quantity of the solute material required for the crystal growth. In the present investigation, the solubility of PCLQI was checked by different combination of organic solvents namely, methanol, ethanol, methanol-chloroform, methanol-acetonitrile, methanol-dichloromethane mixed solvents. From this we optimized that the material has high solubility in methanol-acetonitrile mixed solvent system in the ratio of 3:1. The solubility of purified PCLQI salt was determined for different temperatures from 20 to 40<sup>0</sup>C. The saturated solution for 20<sup>0</sup>C was prepared by continuous stirring to ensure homogeneous temperature and concentration throughout the volume of the solution by using constant temperature water bath with an accuracy of 0.01±<sup>0</sup>C. After attaining saturation, the equilibrium concentration of the solute has been estimated gravimetrically. The same procedure was repeated for other temperatures from 25<sup>0</sup>C to 40<sup>0</sup>C with 5<sup>0</sup>C intervals to determine the equilibrium concentration of the solute. The solubility measurement of PCLQI at different temperatures is shown in Fig. 1. In the graph, it is seen that the solubility of PCLQI linearly increases with increasing temperature. Based on the solubility data, the saturated solution of purified PCLQI was prepared by dissolving it in methanol-acetonitrile (3:1) mixed solvent system at 40<sup>0</sup>C. The resultant solution was filtered in a 150ml beaker and it was covered with aluminium foil. After 10 days good quality seed crystals were obtained and from this one of the seed crystal has been tied up with nylon thread and it was hanged inside the saturated solution. The solution was allowed to slowly evaporate at 40<sup>0</sup>C in a constant temperature water bath. After the evaporation period of 20 days, high quality PCLQI single crystal with dimension of 13 x 4 x 2mm<sup>3</sup> were harvested. The photographs of as grown crystals were shown in Fig.2 (a& b).

The morphology of the grown crystal has been simulated using WinXMorph software program [17]. The CIF data obtained from single crystal XRD data was used as input to predict the morphology of PCLQI single crystal. It is observed that the growth rate of PCLQI elongated along crystallographic b-axis compared to other growth directions. The indexed morphology of grown crystal is shown in Fig. 2c.

### 3. Results and discussion

#### 3.1 Single crystal x-ray diffraction analysis

In order to analyse the crystal structure, the grown PCLQI crystal of dimension (0.2 X 0.2 X 0.15 mm<sup>3</sup>) was subjected to single crystal structure analysis using Rigaku R-AXIS RAPID diffractometer. The Mo-K $\alpha$  radiation ( $\lambda = 0.71075 \text{ \AA}$ ) was used to record the reflections in  $\omega$  scan mode. The crystal structure was solved by the direct methods using SHELX-97[18] and refinement was done by Full matrix least squares technique using the SHELX-97 software program. The crystallographic data and structure refinement details of grown crystal are presented in Table 1. All atoms except hydrogen atoms were refined anisotropically and hydrogen atoms were refined according to the Riding model [19]. From the analysis, PCLQI crystals exhibits monoclinic space group symmetry C2/c with cell parameters  $a = 26.0008(11) \text{ \AA}$ ,  $b = 9.3211(4) \text{ \AA}$ ,  $c = 15.3597(8) \text{ \AA}$ ,  $\beta = 113.3849(14)^\circ$ . The volume of PCLQI crystal system is  $3416.8(3) \text{ \AA}^3$ . The grown crystal crystallizes in centrosymmetric space group, which does not exhibit any second-order NLO properties [20]. Selected bond lengths and bond angles are given in Table 2 and 3, respectively. Fig. 3 exhibits the ORTEP view of PCLQI showing 50% probability displacement ellipsoids.

The asymmetric unit of the title material consists of 2-[2-(4-chloro phenyl)-vinyl]-1-ethyl quinolinium cation (C<sub>19</sub>H<sub>17</sub>ClN<sup>+</sup>), iodide anion (I<sup>-</sup>) and 0.5 water molecule. The cation exists in the trans (*E*) configuration with respect to the C7 = C8 double bond [ $1.340(3) \text{ \AA}$ ] which

can be confirmed by the torsion angle C4-C7-C8-C9 = 178.6 (2)<sup>o</sup>. In crystal packing diagram, the molecules form network chain associated with water molecules and the asymmetric residue viewed down the 'b' axis is shown in Fig. 4. Here the cations are interconnected by water molecules and iodide ions through weak C—H···O and C—H···I interactions to form a three dimensional molecular network. Further, the crystal system is also stabilized by  $\pi$ - $\pi$  interactions between quinolinium and phenyl rings.

The crystallographic information file for PCLQI has been deposited in the Cambridge Crystallographic Data Centre (CCDC# 1446060).

### 3.2 Powder X-ray diffraction analysis

Powder X-ray diffraction analysis were carried out by using Rigaku X-ray diffractometer with Cu-K $\alpha$  radiation ( $\lambda = 1.540598\text{\AA}$ ) to demonstrate the crystallinity of the grown crystal. The sample was recorded over a range of 10-70<sup>o</sup> at a scanning rate of 0.02<sup>o</sup> s<sup>-1</sup>. The various planes of reflections at 2 $\theta$  angles were indexed by using POWDER X software program [21]. The well defined indexed Bragg's peak at specific 2 $\theta$  angles in the powder XRD is shown in Fig. 5. The refined lattice parameters were a = 25.97514  $\text{\AA}$ , b = 9.31059  $\text{\AA}$ , c = 15.3297  $\text{\AA}$ ,  $\beta = 113.402^{\circ}$  crystallizing in monoclinic structure. The appearance of sharp and well- defined peaks proved the good crystalline property of grown crystal PCLQI.

### 3.3 FTIR spectral analysis

In order to confirm the various vibrational modes of functional groups in the grown crystal, FTIR spectrum were recorded in the range of 4000-400cm<sup>-1</sup> using a SHIMADZU IRAFFINITY spectrometer. The measurements were done by using KBr pellet technique and the spectrum is shown in Fig. 6. In FTIR spectrum the peak observed at 3032 and 3074cm<sup>-1</sup> are due to aromatic C- H stretching vibrations and the absorption band at 2949cm<sup>-1</sup> is

assigned to alkyl C- H stretching vibrations. The aromatic C= C stretching vibration of  $\pi$ -conjugated stilbazolium chromophore (C- C= C- C) was confirmed by the peak observed at  $1604\text{cm}^{-1}$ . The sharp peak observed at  $1006\text{cm}^{-1}$  confirms the formation of the title compound by olefinic =C- H bond. The peak at  $1583\text{cm}^{-1}$  is attributed to bending vibration of O- H in water molecule, which may be due to moisture absorbed from atmosphere. The sharp peaks observed at  $1570$  and  $1523\text{cm}^{-1}$  corresponds to the olefinic C- C stretching vibrations. The absorption band around  $1438\text{cm}^{-1}$  corresponds to  $\text{CH}_2$  bending vibrations. The peaks that are observed at  $1377$  and  $1340\text{cm}^{-1}$  are attributed to the ring C- C stretching and ring C- H in-plane bending vibrations. The characteristics vibrational frequencies exhibit between  $480$ - $800\text{cm}^{-1}$  are due to the presence of C- X (X- Br, Cl and F) stretching vibrations [22]. The vibrational frequencies observed in the region  $550$ - $850\text{cm}^{-1}$  can be attributed to the C- Cl stretching vibrations. The peaks observed in the region  $1150$ - $800\text{cm}^{-1}$  can be assigned to the skeletal vibrations of C- C and C- N bonds.

### 3.4 NMR spectral analysis

Nuclear Magnetic Resonance spectroscopy provides the detailed information about molecular structure of synthesized materials and chemical environment of the molecules [23]. The  $^1\text{H}$  NMR for PCLQI was recorded by dissolving the sample in deuterated solvent  $\text{DMSO-d}_6$  using BRUKER instrument operating with a  $400\text{MHz}$  spectrometer. Fig. 7 shows the  $^1\text{H}$  NMR spectra, with the quintet chemical shift at  $2.499\text{ppm}$  assigned to  $\text{DMSO-d}_6$  and water molecule present in  $\text{DMSO-d}_6$  shows chemical shift at  $3.592\text{ppm}$ . Ethyl group attached to the quinolinium ring ( $\text{N-CH}_2\text{-CH}_3$ ) gives a quartet and triplet at  $5.110\text{ppm}$  and  $1.556\text{ppm}$ . The two doublets observed at  $7.565\text{ppm}$  and  $7.808\text{ppm}$  are due to the two olefinic hydrogens ( $\text{CH=CH}$ ). The two doublets at  $9.055$  and  $8.363\text{ppm}$  are corresponds to the hydrogen atom present in the fourth and third position of the  $\text{C}_2\text{H}_5\text{N}$  ring. The triplet signals found at  $8.164$  and  $8.204\text{ppm}$  was caused by hydrogen atoms present in sixth and seventh position of

quinolinium ring. The two doublets observed at 8.542 and 8.565ppm are assigned to protons in the quinolinium ring. Also a chemical shift at 7.991 and 7.940 are attributed to the hydrogen atoms present in the p-substituted benzene ring. In present spectrum the assigned splitting factors for protons present in PCLQI are (400MHz, DMSO-d<sub>6</sub>): 5.11 (q, 2H, J=7.04Hz, NC<sub>2</sub>H<sub>5</sub>), 1.556 (t, 3H, J=7.2Hz, NC<sub>2</sub>H<sub>5</sub>), 7.565 (d, 1H, J=8.8Hz, CH), 7.808 (d, 1H, J=16Hz, CH), 9.055 (d, 1H, J=9.2Hz, C<sub>5</sub>H<sub>2</sub>N), 8.363 (d, 1H, J=7.2Hz, C<sub>5</sub>H<sub>2</sub>N), 8.565 (d, 1H, J=6Hz, C<sub>6</sub>H<sub>4</sub>), 8.542 (d, 1H, J=6.4Hz, C<sub>6</sub>H<sub>4</sub>), 8.164 (t, 1H, J=5.6Hz, C<sub>6</sub>H<sub>4</sub>) 8.204 (t, 1H, J=6Hz, C<sub>6</sub>H<sub>4</sub>), 7.991 (d, 2H, J=8.4Hz, C<sub>6</sub>H<sub>4</sub>) and 7.940 (d, 2H, J=7.6Hz, C<sub>6</sub>H<sub>4</sub>).

The <sup>13</sup>C NMR spectrum of PCLQI is shown in Fig. 8. The peak appearing at 43.89 and 19.40 are due to the presence of ethyl carbon attached to the C<sub>2</sub>H<sub>5</sub>N ring. The signals observed at 124.39 and 133.57ppm are due to the presence of vinyl carbon. The peaks observed at 44.10, 44.31, 44.52, 44.72, 124.18, 126.71, 142.23, 149.86, 150.07ppm are attributed to the quinolinium moiety. Thus the formation of the title compound was confirmed by <sup>1</sup>H NMR and <sup>13</sup>C NMR spectral analysis.

### 3.5 Thermal analysis

The thermo gravimetric analysis (TGA) and differential thermal analysis (DTA) of PCLQI were recorded over a range of 30-500<sup>0</sup>C under nitrogen atmosphere at a heating rate of 10Kmin<sup>-1</sup>. An initial mass of 7.56mg of title material was used to record the TG-DTA which is shown in Fig.9. In TGA curve the initial weight loss of 1.74% illustrates the loss of water molecule and volatile substances in the title material. This is followed by two weight losses, the first step with the weight loss of 41.11% in the temperature range of 230.7<sup>0</sup>C- 254.2<sup>0</sup>C and another weight loss associated with major weight loss 57.15% occurred up to 314.4<sup>0</sup>C. These weight losses attributed to the complete decomposition of PCLQI crystal. In DTA trace, it was observed that the sharp endothermic peak at 239.7<sup>0</sup>C corresponds to the melting

point of PCLQI crystal and this is followed by rapid decomposition at 309.8<sup>0</sup>C. This may due to bulk decomposition of PCLQI crystal and this endotherm coincides with the maximum weight loss of TGA curve. Hence we conclude that the TG-DTA analysis confirms the stability of the material and it can be exploited for any suitable optical applications until its melting point.

### 3.6 Chemical etching studies

Etching of crystal surface provides more information about the surface features, micro structural information, spirals, hillocks, and slip patterns on the growing crystal surface. Etch patterns observed on crystal surface provides detailed information of the growth process and growth mechanism of the crystal [24]. In present investigation, Etching studies were carried out for PCLQI crystal using methanol-acetonitrile (3:1) as etchant for a time period of 15s and 30s. The crystal surface was examined using a Carl zies optical microscope in reflection mode. The surface micrograph of as grown crystal is shown in Fig.10 (a-c). Fig. 10a shows the before etch pattern of the as grown PCLQI crystal. Fig. 10b shows well defined rectangular etch pits for 15s. When increasing the etch time 15s to 30s, the size of the etch pits also elongated as shown in Fig. 10c. The observed etch patterns due to the layer growth, confirmed the two-dimensional mechanism with fewer dislocations [25].

### 3.7 Optical absorption spectral analysis

The optical absorption spectrum of PCLQI was recorded in the range of 200-1100nm using a Perkin Elmer UV spectrophotometer. The UV-vis-NIR spectra of PCLQI crystal exhibit maximum cut-off wavelength at 485nm, which is attributed to  $\pi$ - $\pi^*$  transition due to the presence of conjugated system in the PCLQI molecule. Optical switching application has required finding a high third order nonlinear optical material, as well as large transmittance or low absorption in near IR region. Fig. 11 shows the UV absorption spectrum of PCLQI single

crystal of 1mm thickness. No absorption band observed in the region between 485-1100nm and it has very good optical transparency in near infrared region. The measured absorption values of PCLQI crystal was used to calculate the absorption coefficient ( $\alpha$ ) by using the equation [26],

$$\alpha = \frac{2.303 \log A}{t} \quad (1)$$

Where A is the absorption and t is the thickness of the sample. The optical absorption coefficient has been used to calculate the energy band gap of the material. The optical band gap was calculated by using the relation,

$$\alpha h\nu = A (E_g - h\nu)^2 \quad (2)$$

The graph is plot between photon energy ( $h\nu$ ) versus  $(\alpha h\nu)^2$  and the energy band gap is figured out by extrapolating the linear part from the maximum absorption end to the photon energy axis as shown in Fig. 12. The Tauc's method has been used to measure the optical band gap of PCLQI crystal and it is found to be 2.15eV. Thus the large transmittance near IR region and low energy gap of this crystal proves that it is a potential candidate for used in optical devices such as optical switching and various nonlinear optical applications.

### 3.8 Z-scan studies

The Third order optical property of PCLQI crystal has been investigated using Z-Scan technique and it is a accurate method to determine the sign and magnitude of nonlinear refractive index and nonlinear absorption coefficient developed by Sheik Bahae et al [27]. Here the open aperture and closed aperture Z scan is used for nonlinear absorption coefficient and nonlinear refractive index measurements and this method has been widely accepted by nonlinear optics community due to its simplicity and high sensitivity. In this experiment, He-Ne laser (632.8 nm) with the input intensity of 5mW used for sample excitation, and its

propagation direction is taken as Z-axis. The Gaussian beam was focused using a convex lens (30mm), and the focal point is taken as  $Z = 0$ . The thickness of the sample is very important to minimize the phase transition, for this a sample thickness 0.7mm was used. Thus the essential criteria of Rayleigh length ( $Z_0 < L$ ) were found to be satisfied and it can be calculated by using the formula  $Z_0 = K\omega_0^2/2$ , where  $K$  is  $2\pi/\lambda$  and  $\omega_0$  is the radius of the focal length. The maximum energy density of the beam is at the focus, which is being symmetrically reduced both sides for the positive and negative values of  $z$ , this leads to the difference in laser intensity at different  $z$  positions. The transmittance intensity variations corresponding to the  $z$  values, the open aperture and closed aperture  $z$ -scan curve can be drawn. The recorded normalized transmittance for PCLQI crystal is shown in Fig. 13 and Fig. 14. The sample can act as a thin lens of variable focal length, as the sample brought closer to the focus, the irradiance of Gaussian beam increases or decreases depending upon the material absorption and refractive index. From open aperture method, the nonlinear absorption coefficient can be easily calculated from maximum or minimum transmittance curves. It was observed that, the sample transmittance increases while increasing the input intensity of laser beam, which demonstrates the absence of reverse saturation absorption (RSA) with enhanced strong saturation absorption (SA) in PCLQI crystal. From the closed aperture curve, the prefocal valley to post focal peak configuration clearly suggests that the title crystal has a positive sign of third order nonlinear refractive index and this behaviour attributed to self focusing effect. This may caused by reduced transmittance and large beam divergence through the far field aperture, which is an essential property for optical switching applications [28]. The magnitude of third order nonlinear optical susceptibility ( $\chi^{(3)}$ ) has been calculated by using the formula,

$$|\chi^{(3)}| = [(\text{Re}(\chi^{(3)}))^2 + (\text{Im}(\chi^{(3)}))^2]^{1/2} \quad (3)$$

The real and imaginary part of third order susceptibility can be defined as [29],

$$\text{Re}(\chi^{(3)})(\text{esu}) = \frac{10^{-4}(\epsilon_0 C^2 n_0^2 n_2)}{\pi} (\text{cm}^2 \text{W}^{-1}) \quad (4)$$

$$\text{Im}(\chi^{(3)})(\text{esu}) = \frac{10^{-2}(\epsilon_0 C^2 n_0^2 \lambda \beta)}{4\pi^2} (\text{cm} \text{W}^{-1}) \quad (5)$$

In closed aperture method, on axis phase shift ( $\Delta\Phi$ ) is calculated from the difference between the transmittance change of peak and valley and the equation of on axis phase shift ( $\Delta\Phi$ ) is in terms of normalised transmittance can be defined as  $\Delta T_{P-V} = 0.406(1-S)^{0.25} |\Delta\Phi|$  [30], where S is the aperture linear transmittance ( $S=2$ ) and it can be calculated by using the relation,  $S = 1 - \exp[-2r_a/\omega_a^2]$ . Where  $r_a$  is the radius of aperture and  $\omega_a$ , is the beam radius at the aperture. The third order nonlinear refractive index of the crystal can be studied in terms of on-axis phase shift [31],

$$n_2 = \Delta\Phi / K I_0 L_{\text{eff}} \quad (6)$$

Here  $L_{\text{eff}}$  is an effective thickness of the crystal was calculated using the following relation,  $L_{\text{eff}} = 1 - \exp(-\alpha L) / \alpha$ . In open aperture method, the nonlinear absorption coefficient ( $\beta$ ) has been estimated from the relation [32],

$$\beta = 2\sqrt{2} \Delta T / I_0 L_{\text{eff}} \quad (7)$$

The negative nonlinear absorption has been observed in PCLQI single crystal due to strong saturation absorption in the material. The obtained values of third order nonlinear refractive index and nonlinear absorption coefficient are  $1.56 \times 10^{-11} \text{ m}^2 \text{W}^{-1}$  and  $1 \times 10^{-4} \text{ mW}^{-1}$  respectively. The third order nonlinear susceptibility of grown crystal is  $4.5226 \times 10^{-6} \text{ esu}$  and it can be related with the second order molecular hyperpolarizability. The molecular second order hyperpolarizability of PCLQI crystal estimated by using the following equation,

$$\text{Re}(\gamma) = \text{Re}(\chi_3) / N f^4 \quad (8)$$

Here  $N$  is number of molecules per unit volume and  $f$  is the local field correction factor according to Lorentz equation,

$$f = (n_o^2 + 2)/3 \quad (9)$$

Generally third order optical property of materials is related with all optical switching applications. To know the suitability of grown crystal for all optical switching applications, two figures of merit,  $W$  and  $T$  have been calculated from obtained third order optical parameters. For all optical switching application, a values  $W \gg 1$  and  $T \ll 1$  should be needed [33]. For PCLQI crystal the values have been calculated to be  $17 \gg 1$  and  $0.405 \ll 1$ , which satisfies the requirement of all switching applications. The Z-scan experiment indicates that the PCLQI single crystal exhibit high nonlinearity for optical application and the calculated parameters of the title crystal are tabulated in Table. 4. The third order optical property of PCLQI crystal is compared with some other organic crystals tabulated in Table. 5. The large value of  $\chi^3$  can be attributed to high density  $\pi$ - electron cloud within the quinolinium molecular system [34]. Therefore, the polarization of the  $\pi$ -conjugated electrons in the quinolinium molecular system will be high and it will contribute to the large value of  $\chi^3$  and  $\gamma$ . Thus, the obtained results show that PCLQI crystal has an excellent potential material for all optical switching and third order optical applications.

#### 4. Conclusion

A quinolinium derived single crystal PCLQI were synthesized and grown by slow evaporation technique. Single crystals of size with  $13 \times 4 \times 2\text{mm}^3$  were grown and morphology of the grown crystal was determined by using WinXmorph program. The

structure of the grown crystal were determined and refined single crystal XRD using SHELX-97 software program and the obtained lattice parameters were  $a = 26.0008 (11) \text{ \AA}$ ,  $b = 9.3211 (4) \text{ \AA}$ ,  $c = 15.3597 (8) \text{ \AA}$  and  $\beta = 113.3849 (14)^\circ$ . The crystalline perfection was studied by powder XRD and it confirms the crystalline nature of the PCLQI crystal is fairly good. The presence of functional groups and structure of title material was confirmed by FTIR and NMR spectral analysis. Thermal behaviour of PCLQI was studied by TG/DTA analysis and thermally stable up to its melting point. The UV-vis-NIR spectrum shows that the cut-off wavelength is found to be 485nm and the lower value of optical band gap (2.15eV) was obtained by plotting of Tauc's plot. The third order optical property of grown crystal reveals that it possesses large nonlinear absorption coefficient ( $\beta = 1 \times 10^{-4} \text{ mW}^{-1}$ ) and third order optical susceptibility, which enhances the suitability of grown title crystal for all optical switching applications. Thus from the above studies suggests that the grown PCLQI crystal is a new candidate for Third order optical applications.

### References:

1. Blanca Ruiz, Zhou Yang, Volker Gramlich, Mojca Jazbinsek and Peter Gunter., J. Mater. Chem., 2006, 16, 2839–2842.
2. S. Suresh, D. Arivouli., J. Optoelectron. Bio. Med. Mater., 2011, 3, 63–68.
3. B. Ferguson, X.C. Zhang, Nat. Mater., 2002, 1, 26.
4. M. Jazbinsek, O. P. Kwon, Ch. Bosshard and P. Gunter, in Handbook of Organic Electronic and Photonics, ed. S. H. Nalwa, American Scientific Publishers, Los Angeles, 2008, ch.1.
5. Pil-Joo Kim, Mojca Jazbinsek, Jae-Hyeok Jeong, Jong-Taek Kim, Yoon Sup Lee, Yeong-Min Jung, Soon W. Lee and O-Pil Kwon CrystEngComm, 2012, 14, 3633.

6. B. J. Coe, J. A. Harris, I. Asselberghs, K. Wostyn, K. Clays, A. Persoons, B. S. Brunshwig, S. J. Coles, T. Gelbrich, M. E. Light , M. B. Hursthouse and K. Nakatani, *Adv. Funct. And Mater*, 2003, 13, 347.
7. Ji-Soo Kim, Jae-Hyeok Jeong, Hoseop Yun, Mojca Jazbinsek, Jun Wan Kim, Fabian Rotermund, and O-Pil Kwon, *Cryst.Growth Des*, 2013,13, 5085- 5091.
8. Z. Yang, S. Aravazhi, A. Schneider, P. Seiler, M. Jazbinsek, P. Gunter, *Synthesis andcrystal growth of stilbazolium derivatives for second-order nonlinear optics*,*Adv. Funct. Mater*, 2005, 15, 1072–1076.
9. Pumsak Ruanwas, Tawanrat Kobkeatthawin, Suchada Chantrapromma, Hoong-Kun Fun, Reji Philip, N. Smijesh, Mahesh Padaki, Arun M. Isloor, *Synthetic Metals* 160 (2010) 819–824.
10. Jae-Hyeok Jeong, Ji-Soo Kim, Jochen Campo, Seung-Heon Lee , Woo-Yong Jeon , Wim Wenseleers , Mojca Jazbinsek, Hoseop Yun , O-Pil Kwon, *Dyes and Pigments*, 2015, 113, 8-17.
11. Vladimir Burtman, Anna Teplitsky and Alexander Zelichenok., *Tetrahedron Letters*, 2000, 41, 5397-5402.
12. Jeong JH, Kang BJ, Kim JS, Jazbinsek M, Lee SH, Lee SC, et al. *Sci Rep*, 2013, 3, 3200.
13. Lee SH, Jazbinsek M, Yun H, Kim JT, Lee YS, Kwon OP., *Dyes Pigments*, 2013, 96(2), 435-9.
14. Kim PJ, Jeong JH, Jazbinsek M, Choi SB, Beak IH, Kim JT, et al.,*Adv Funct Mater.*, 2012, 22(1), 200-9.
15. Boonwasana Jindawong, Suchada Chantrapromma, Hoong-kun Fun, Chatchanok karalai, *ActaCryst.*, 2005, E61, 03237-03239.

16. J.L.Bredas, C. Adant, P. Tackx, A. Persoons, B.M. Pierec, *Chem. Rev.* 1994, 94 (1), 243-278.
17. W. J. Kaminsky, *J. Appl. Crystallogr.*, 2007, 40, 382.
18. G.M. Sheldrick, *Acta Cryst.*, 2008, A64, 112-122.
19. Jens Lubben, Christian Volkmann, Simon Grabowsky, Alison Edwards, Wolfgang Morgenroth, Francesca P. A. Fabbiani, George M. Sheldrick and Birger Dittrich., *Acta Cryst*, 2014, A70, 309–316.
20. Suchada Chantrapromma, Thawanrat Kobkeathawin, Kullapa Chanawanno, Chatchanok Karalai and Hoong-Kun Fun, 2008, E64, 876-877.
21. C.Dong, *J. Appl. Crystallogr.*, 1999, 32, 4.
22. M. K. Murali, V. Balachandran, M. Murugan, M. Karnan., *Journal of Basic and Applied Physics*, 2012, 1, 79-88.
23. R.Jeraldvijay, N.Melikechi, Tina Thomas, R.Gunaseelan, M.AntonyArockiaraj, P.Sagayaraj.,*J. Cryst. Growth*, 2012, 338, 170-176.
24. G. Pabitha, R. Dhanasekaran., *J. Cryst. Growth*, 2013, 362, 259–263.
25. S. Mukerji, T. Kar., *J. Cryst.Growth*, 1999, 204,341–347.
26. A. Silambarasan, P. Rajesh, P. Ramasamy., *Spectrochimica Acta Part A: Molecular and Biomolecular Spectroscopy.*, 2014, 118, 24–27.
27. M. Sheik Bahae, A.A. Said, T.M.Wei, D.J. Hagan, E.W. Vanstryland, *IEEE J. Quant.Electron*, 1990, 26, 760.
28. D.Bharath. S.Kalainathan., *Opt.laser Technol.*, 2014, 59, 24-31.
29. R.N. Shaikh, M.D.Shirsat, P.M.Koinka, S.S.Hussaini., *Opt. laser Technol.*, 2015, 69, 8–12.
30. T.Kanagasekaran, p.Mythili, P.srinivasan, A.Y.Nooraldeen, P.K.Palanisamy and R.Gopalakrishnan, *Cryst. GrothDes*, 2008, 8, 2335-2339.

31. S.Karthiga, S.Kalainathan, KundaUma Maheswara Rao, FumioHamada, Manabu Yamada, Yoshihikokondo., *J. Cryst. Growth*, 2016, 436, 113-124.
32. P. Nagapandiselvi, C. Baby and R. Gopalakrishnan, *RSC Adv.*, 2014, 4, 22350–22358.
33. J. Sun, W. F. Guo, X. Q. Wang, G. H. Zhang, X. B. Sun, L. Y. Zhu, Q. Ren and D. Xu, *Opt. Commun.*, 2007, 280, 183–187.
34. Y. S. Zhou, E. B. Wang, J. Peng, J. Liu, C. W. Hu, R. D. Huang and X. You, *Polyhedron*, 1999, 18, 1419–1423.
35. M.K.Kumar, S.Sudhahar, A.Silambarasan, B.M.Sornamurthy, R.M.Kumar, *Optik.*, 2014, 125, 751–755.
36. M. Krishna Kumar, S. Sudhahar, P. Pandi , G. Bhagavannarayana , R. Mohan Kumar, *Optical Materials.*, 2014, 36, 988–995.

## LIST OF FIGURES:

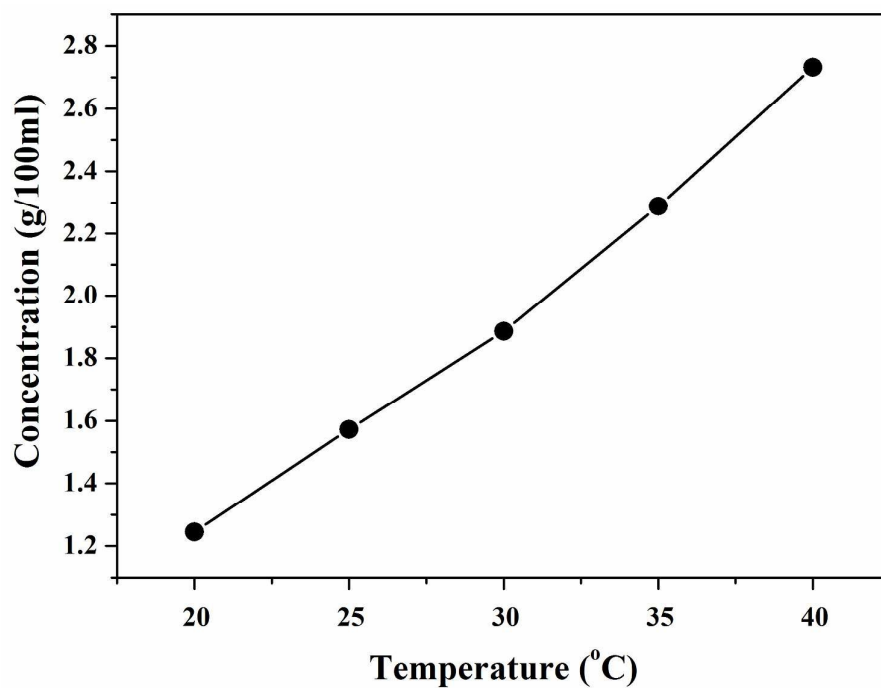


Fig.1 solubility curve of PCLQI in Methanol-Acetonitrile solvent system

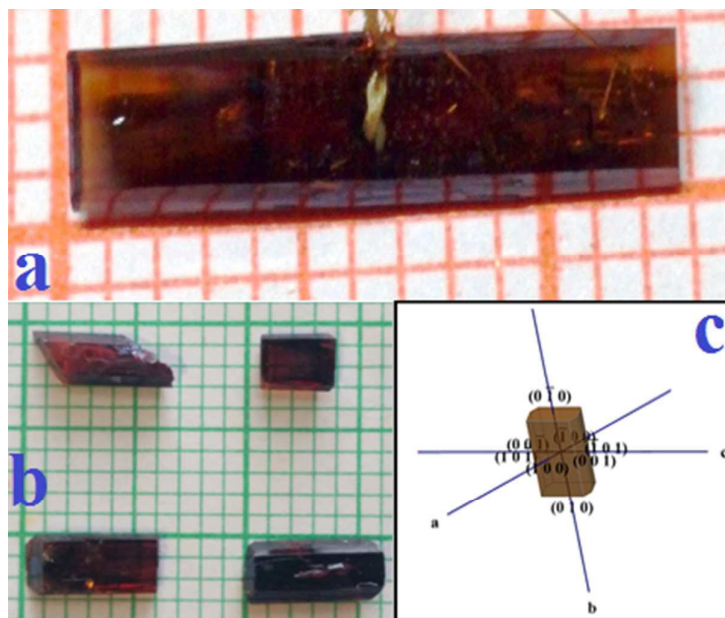
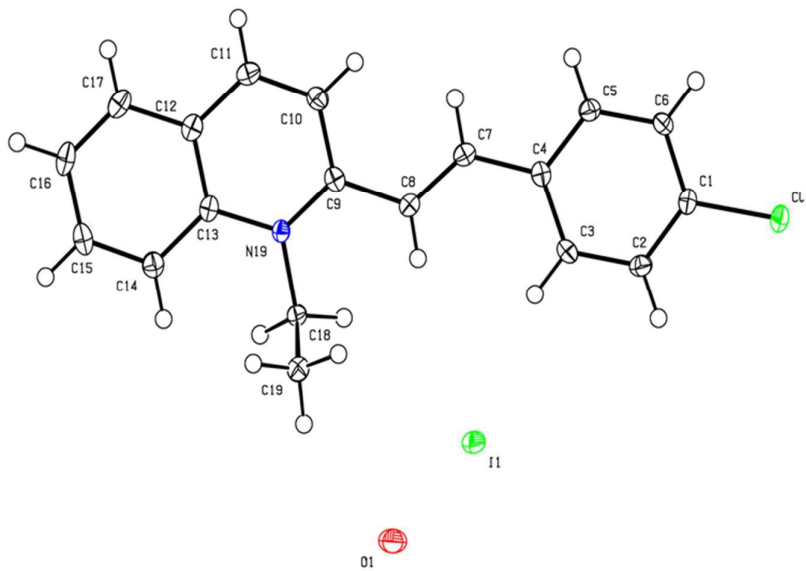
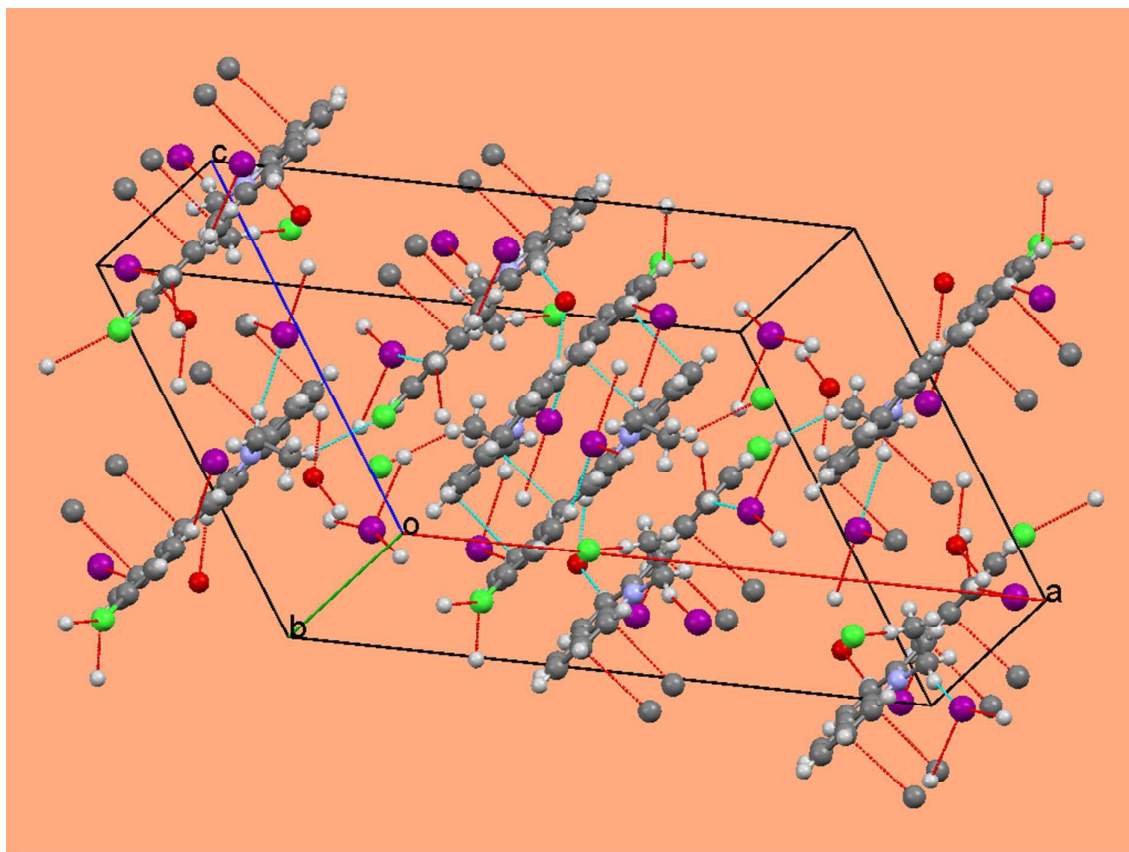


Fig.2 Photograph of as grown PCLQI crystals



**Fig.3** ORTEP view of PCLQI



**Fig.4** Crystal packing diagram of PCLQI

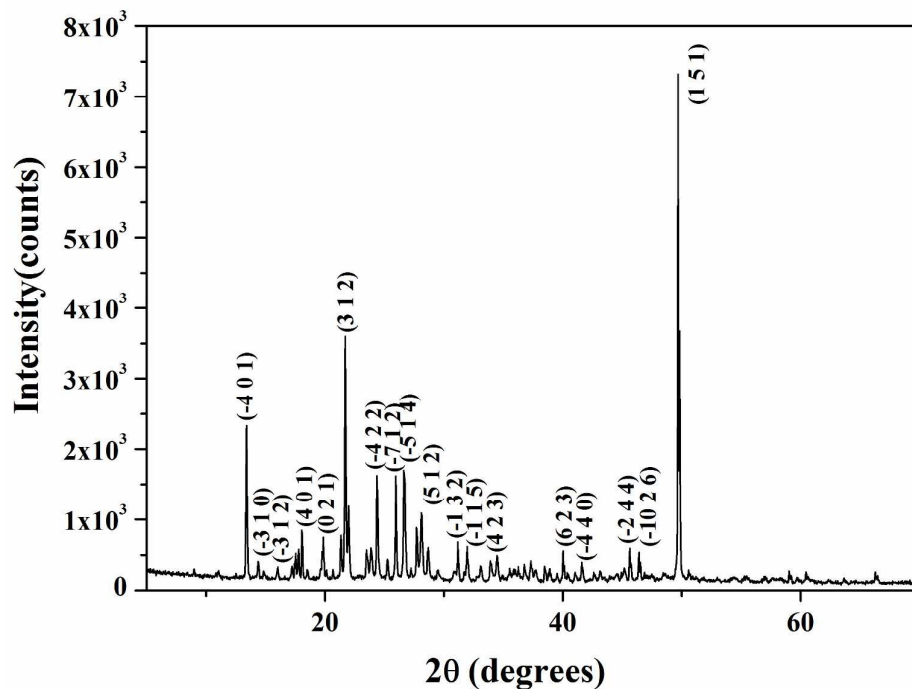


Fig.5 Powder XRD pattern of PCLQI

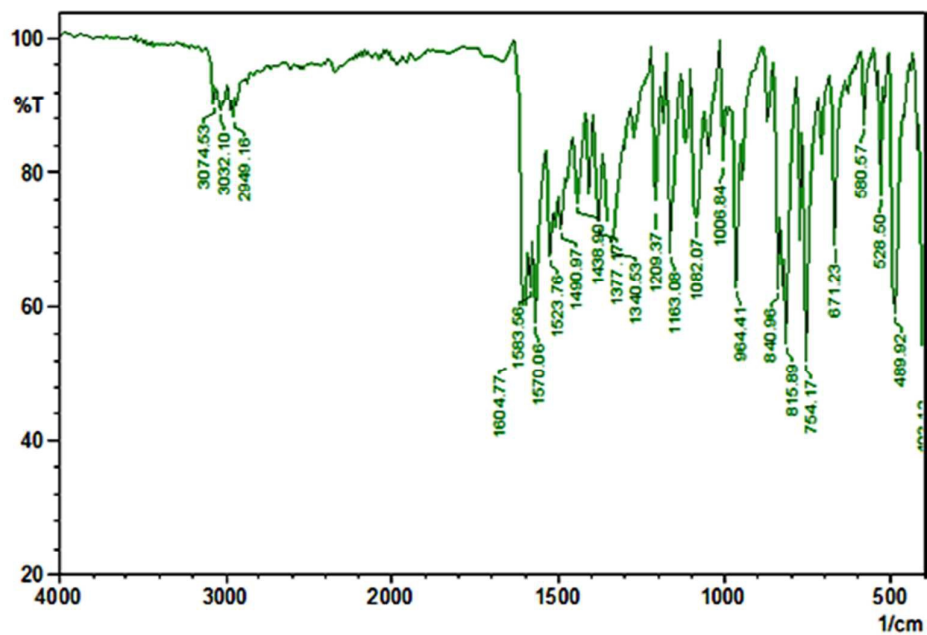
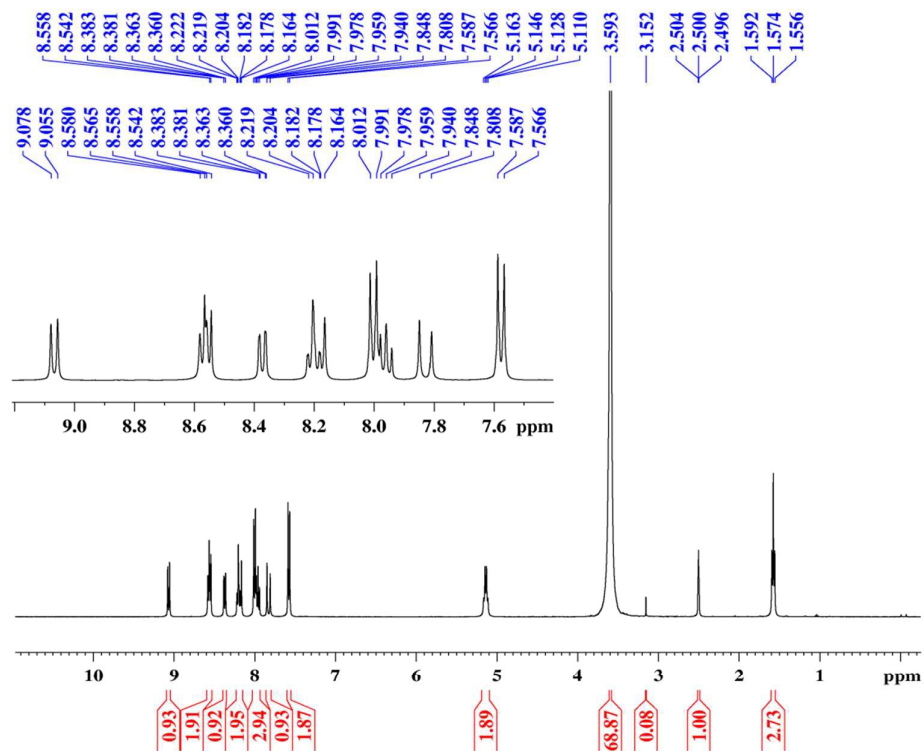
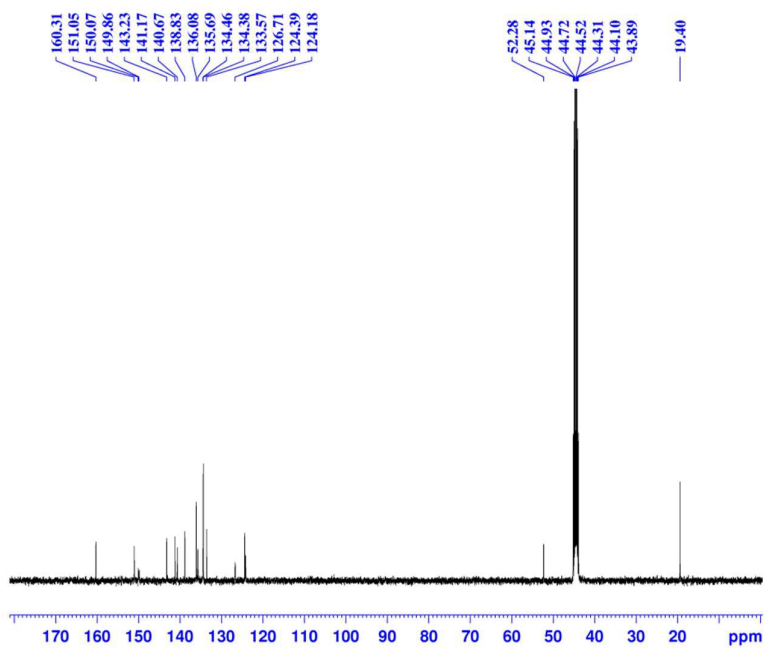


Fig.6 FTIR spectrum of PCLQI

Fig.7  $^1\text{H}$  NMR spectrum of PCLQIFig.8  $^{13}\text{C}$  NMR spectrum of PCLQI

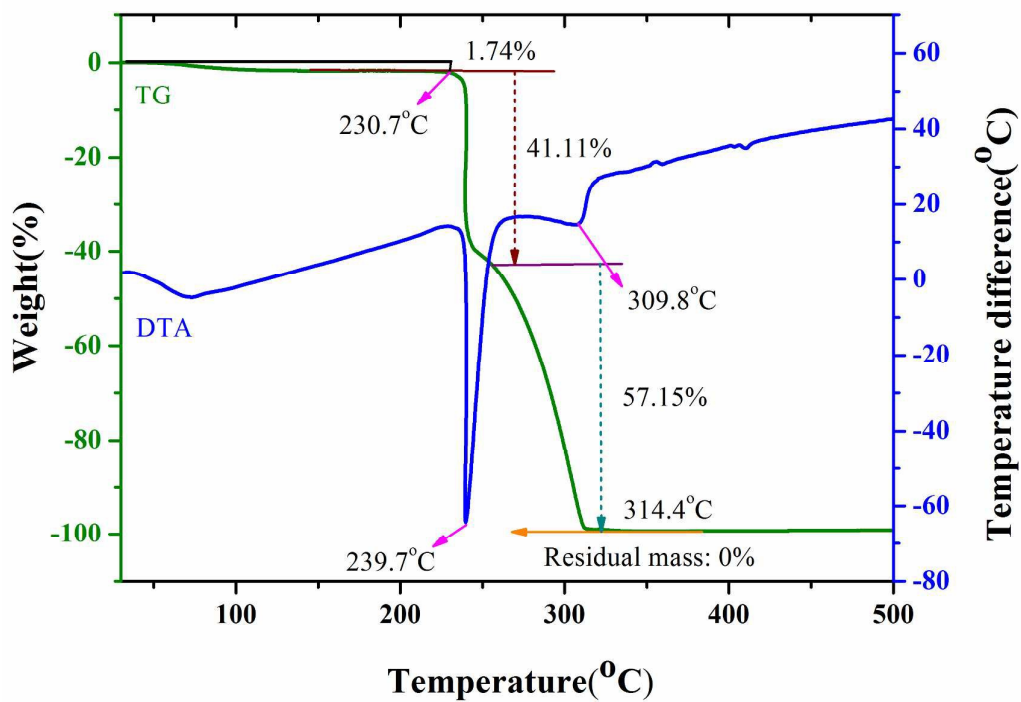
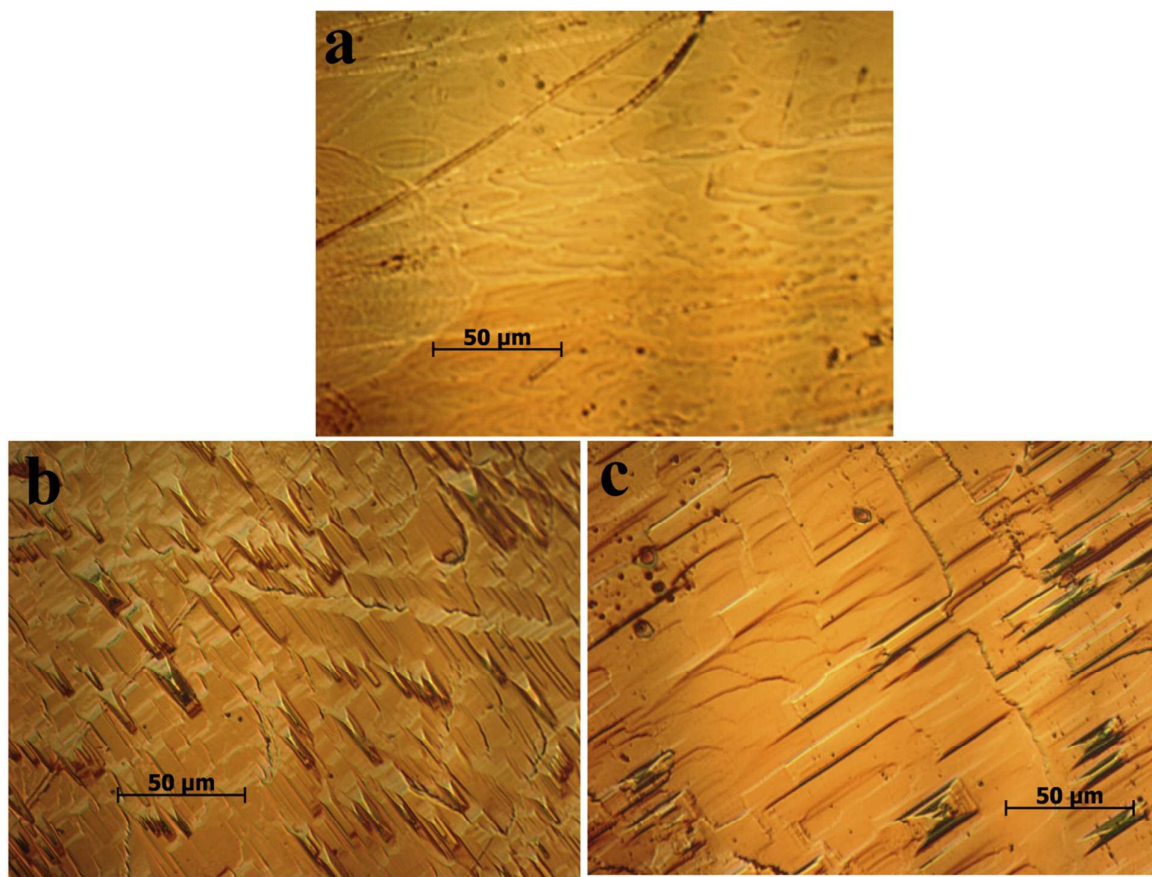


Fig.9 TG&DTA curves of PCLQI



**Fig.10 Etch pit patterns of PCLQI crystal with Methanol – Acetonitrile as etchant**

**(a)Before etching (b) 10s (c) 20s**

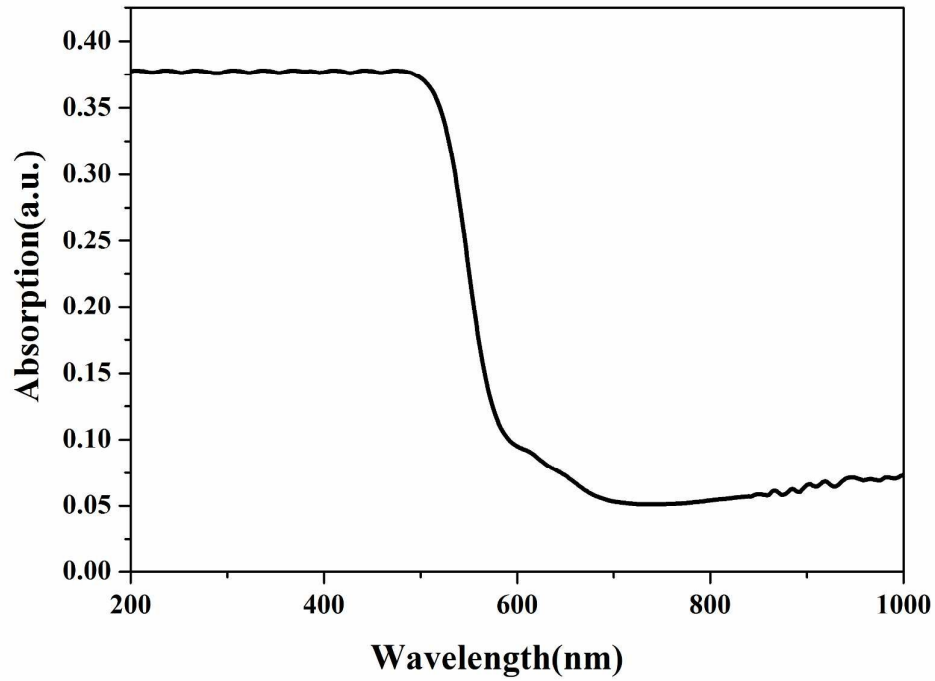


Fig.11 Absorption spectrum of PCLQI crystal

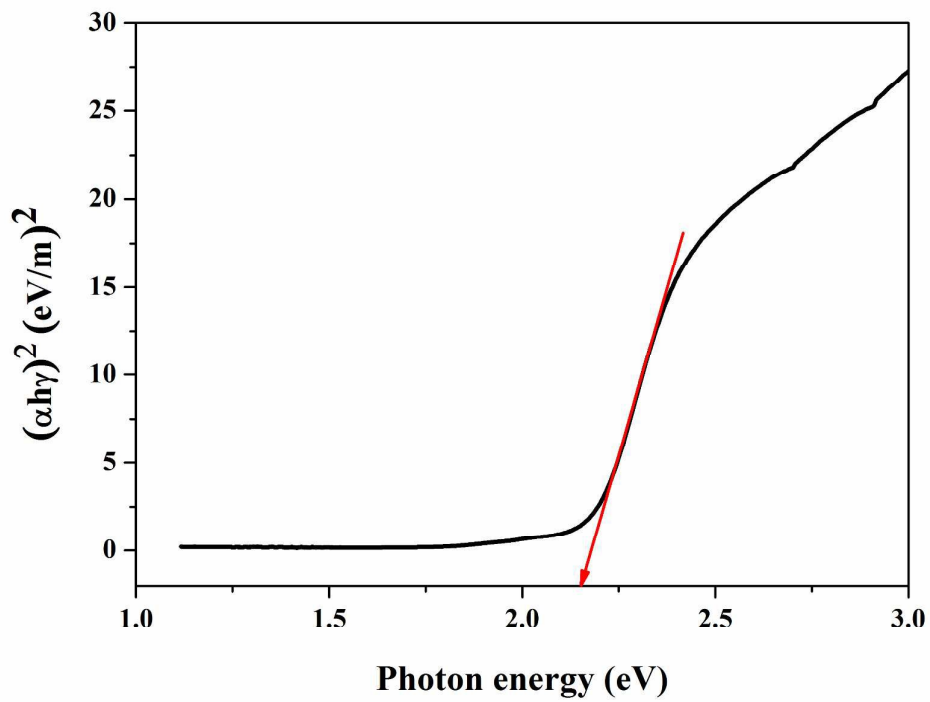


Fig.12 Tauc's plot for 4CLNS crystals

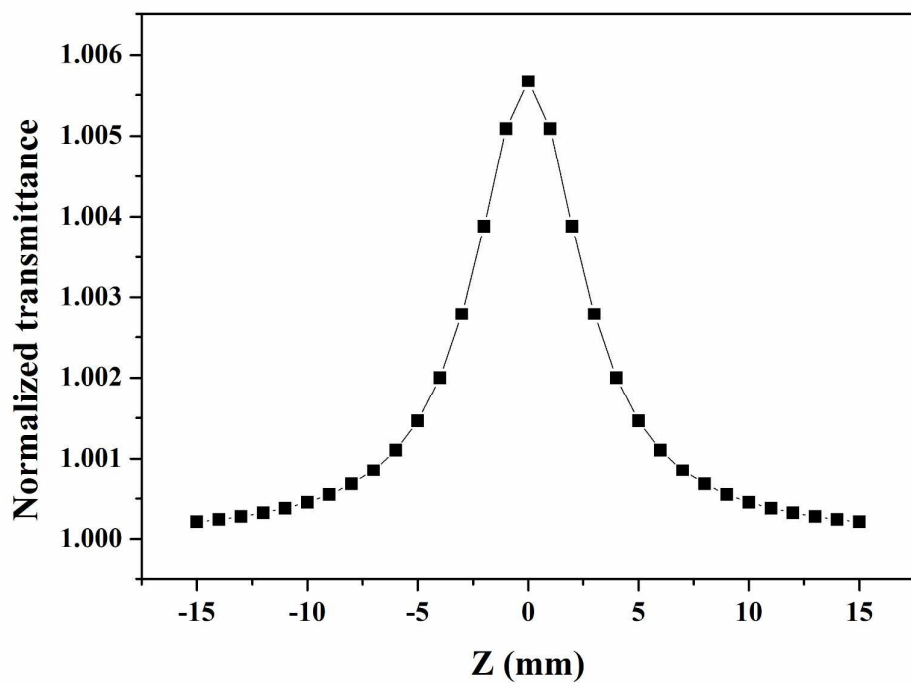


Fig.13 Open aperture spectrum of PCLQI crystal

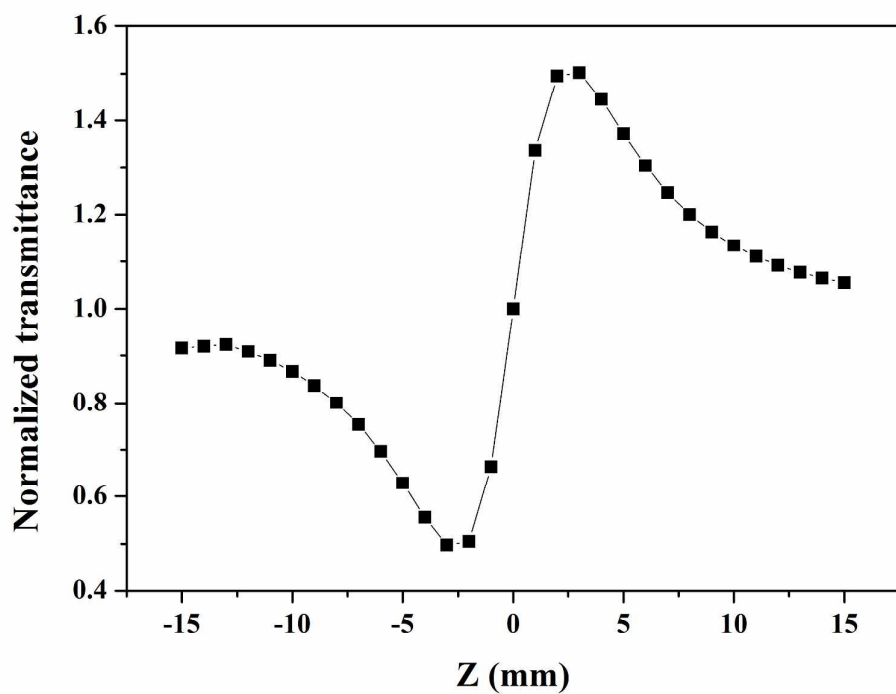


Fig.14 Closed aperture spectrum of PCLQI crystal

TABLE CAPTION:

TABLE 1

Crystal data and structure refinement for PCLQI

Empirical formula	$C_{38}H_{34}Cl_2N_2I_2O$
Formula weight	859.41
Temperature	100K
Wavelength	0.71075Å
Crystal system	Monoclinic
Space group	$C_2/C$
Unit cell dimensions	$a = 26.0008(11) \text{ \AA}$ $\alpha = 90^\circ$ $b = 9.3211(4) \text{ \AA}$ $\beta = 113.3849(14)^\circ$ $c = 15.3597(8) \text{ \AA}$ $\gamma = 90^\circ$
Volume	$3416.8(3) \text{ \AA}^3$
Z	4
Density	$1.671 \text{ g/cm}^3$
Absorption coefficient	$2.033 \text{ mm}^{-1}$
F(000)	1690
Crystal size	$0.2 \times 0.2 \times 0.1 \text{ mm}^3$
Theta range for data collection	$0.0^\circ$ to $25.33^\circ$
Reflections collected	13310
Unique reflections	3119 [R(int) = 0.0223]
Completeness to theta= $25.33^\circ$	99.7%
Max. and min. transmission	0.737 and 0.595
Refinement method	Full matrix least square on $F^2$
Data/ restraints/ parameters	3119/ 0 /212
R indices (all data)	$R_1 = 0.0165$ , $W R_2 = 0.0414$
Goodness-of -fit on $F^2$	1.082
Largest diff. Peak and hole	0.65 and $-0.31 \text{ e. \AA}^{-3}$

Table 2:

Bond length (Å) for PCLQI crystal

Atom	Atom	Length	Atom	Atom	Length
C11	C1	1.7432(16)	N19	C9	1.356(3)
N19	C13	1.402(2)	N19	C18	1.494(3)
C1	C2	1.391(3)	C1	C6	1.385(3)
C2	C3	1.390(3)	C3	C4	1.398(3)
C4	C5	1.400(3)	C4	C7	1.465(3)
C5	C6	1.388(2)	C7	C8	1.340(3)
C8	C9	1.463(3)	C9	C10	1.413(3)
C10	C11	1.359(3)	C11	C12	1.408(3)
C12	C13	1.413(3)	C12	C17	1.415(3)
C13	C14	1.412(3)	C14	C15	1.379(3)
C15	C16	1.404(3)	C16	C17	1.365(3)
C18	C19	1.512(4)			

Table 3:

Bond angles (°) for PCLQI crystal

Atom	Atom	Atom	Angle	Atom	Atom	Atom	Angle
C9	N19	C13	121.54(16)	C9	N19	C18	120.87(13)
C13	N19	C18	117.59(14)	C11	C1	C2	119.50(14)
C11	C1	C6	118.93(18)	C2	C1	C6	121.57(15)
C1	C2	C3	119.03(18)	C2	C3	C4	120.62(17)
C3	C4	C5	118.96(15)	C3	C4	C7	123.44(16)
C5	C4	C7	117.60(16)	C4	C5	C6	120.93(17)
C1	C6	C5	118.87(16)	C4	C7	C8	127.35(18)
C7	C8	C9	122.47(18)	N19	C9	C8	120.35(17)
N19	C9	C10	118.97(14)	C8	C9	C10	120.67(16)
C9	C10	C11	121.08(16)	C10	C11	C12	120.35(18)
C11	C12	C13	118.71(15)	C11	C12	C17	121.82(18)
C13	C12	C17	119.45(17)	N19	C13	C12	119.04(15)
N19	C13	C14	121.58(17)	C12	C13	C14	119.37(15)
C13	C14	C15	119.07(19)	C14	C15	C16	121.99(18)
C15	C16	C17	119.25(17)	C12	C17	C16	120.80(19)
N19	C18	C19	112.09(18)				

Table 4:

Obtained non linear optical parameters from Z scan measurements for PCLQI crystal

Laser beam wavelength ( $\lambda$ )	632.8nm
Lens focal length (f)	30mm
Optical path length	85cm
Beam radius of the aperture ( $w_a$ )	3.3mm
Aperture radius ( $r_a$ )	2mm
Sample thickness (L)	0.7mm
Effective thickness ( $L_{eff}$ )	0.6778mm
Linear absorption coefficient ( $\alpha$ )	0.3686
Linear transmittance (S)	0.15
Nonlinear refractive index ( $n_2$ )	$1.56 \times 10^{-11} \text{ m}^2\text{W}^{-1}$
Nonlinear absorption coefficient ( $\beta$ )	$1 \times 10^{-4} \text{ mW}^{-1}$
Real part of third order susceptibility [ $\text{Re}(\chi_3)$ ]	$4.3033 \times 10^{-6} \text{ esu}$
Imaginary part of third order susceptibility [ $\text{Im}(\chi_3)$ ]	$1.3915 \times 10^{-6} \text{ esu}$
Third order nonlinear susceptibility ( $\chi_3$ )	$4.5226 \times 10^{-6} \text{ esu}$
Second order molecular hyperpolarizability ( $\gamma$ )	$1.61521 \times 10^{-33} \text{ esu}$

Table 5:

Comparison of  $\chi_3$  with some organic crystals

S.no	Crystal	Third order optical susceptibility ( $\chi_3$ )	References
1	4CLNS	$4.8565 \times 10^{-5} \text{ esu}$	[31]
2	PCLQI	$4.5226 \times 10^{-6} \text{ esu}$	Present work
3	MMST	$2.29 \times 10^{-7} \text{ esu}$	[35]
4	VMST	$9.6963 \times 10^{-12} \text{ esu}$	[36]